

# Raman Spectroscopy for Quantitative Analysis in the Pharmaceutical Industry

José Izo Santana da Silva de Jesus<sup>1</sup>, Raimar Löbenberg<sup>2</sup>, Nádia Araci Bou-Chacra<sup>1</sup>

<sup>1</sup>Department of Pharmacy, Faculty of Pharmaceutical Sciences, University of São Paulo, Professor Lineu Prestes Av 580, Cidade Universitária, 05508-000 São Paulo, SP, Brazil. <sup>2</sup>Faculty of Pharmacy and Pharmaceutical Sciences, Katz Group-Rexall Centre for Pharmacy & Health Research, University of Alberta, Edmonton, Alberta, Canada.

Received, July 24, 2019; Revised, October 27, 2019; Accepted, January 3, 2020; Published, February 27, 2020.

**ABSTRACT** - Raman spectroscopy is a very promising technique increasingly used in the pharmaceutical industry. Due to its development and improved instrumental versatility achieved over recent decades and through the application of chemometric methods, this technique has become highly precise and sensitive for the quantification of drug substances. Thus, it has become fundamental in identifying critical variables and their clinical relevance in the development of new drugs. In process monitoring, it has been used to highlight in-line real-time analysis, and it has been used more commonly since 2004 when the Food and Drug Administration (FDA) launched Process Analytical Technology (PAT), integrated with the concepts of Pharmaceutical Current Good Manufacturing Practices (CGMPs) for the 21<sup>st</sup> Century. The present review presents advances in the application of this tool in the development of pharmaceutical products and processes in the last six years.

## INTRODUCTION

Raman and Krishnan discovered Raman spectroscopy in 1928, and this technique has gone several breakthroughs between the 1930s and 1950s. Currently, it is one of the leading analytical techniques among spectroscopies (1–3). This technique, based on light scattering during monochromatic radiation exposure to samples, involves molecular vibration of the chemical structures of a substance (1,4).

The monochromatic laser beam illuminates the samples resulting in scattered light, from photon-molecule interactions. Each photon occurs in a different vibrational mode, and this frequency difference refers to the separation of the vibrational energy level of the molecules. The dispersion signals origins from the inelastic movement between the incident monochromatic radiation and vibrational molecular motions, providing a unique signature for each substance (1,4–6).

In the pharmaceutical industry, Raman spectroscopy is an excellent tool for identifying counterfeit drugs (1,7). In addition, it is suitable in product development and the real-time monitoring of productive processes through Process Analytical Technology (PAT), according to the current concepts of Pharmaceutical Current Good Manufacturing Practices (CGMPs) for the 21<sup>st</sup> Century (1,8).

Raman spectroscopy has essential advantages due to its non-invasive feature; it does not use

solvents; it is easy to use, and the analyses can be without any preparation, even penetrating primary packaging, such as polymeric materials and transparent glasses. In addition, portable types of equipment are available, and the analytical results can be obtained in seconds (1,8).

Therefore, this review presents the advances of Raman spectroscopy application in the quantitative analyses in the product development cycles and as a tool in process analytical technology (PAT).

## Main variants of Raman spectroscopy

In addition to the conventional Raman dispersion phenomenon, several studies, over recent decades, have made possible the discovery of other events, which allowed the development of several variants of this spectroscopy (1,4,6). The difference frequency of incident radiation and the intensity of the dispersion signals originates Stokes and anti-Stokes lines, as shown in Figure 1. These phenomena define the basic principle for the variants presented in Table 1 (5,9). The instrumental versatility of Raman spectroscopy includes interferometric dispersive systems, single channel multichannel detection systems, and microscope coupled systems (Table 1). Several laser systems are available for

**Corresponding Author:** Nádia Araci Bou-Chacra, Department of Pharmacy, Faculty of Pharmaceutical Sciences, University of São Paulo, Professor Lineu Prestes Av 580, Cidade Universitária, 05508-000 São Paulo, SP, Brazil; E-mail: chacra@usp.br

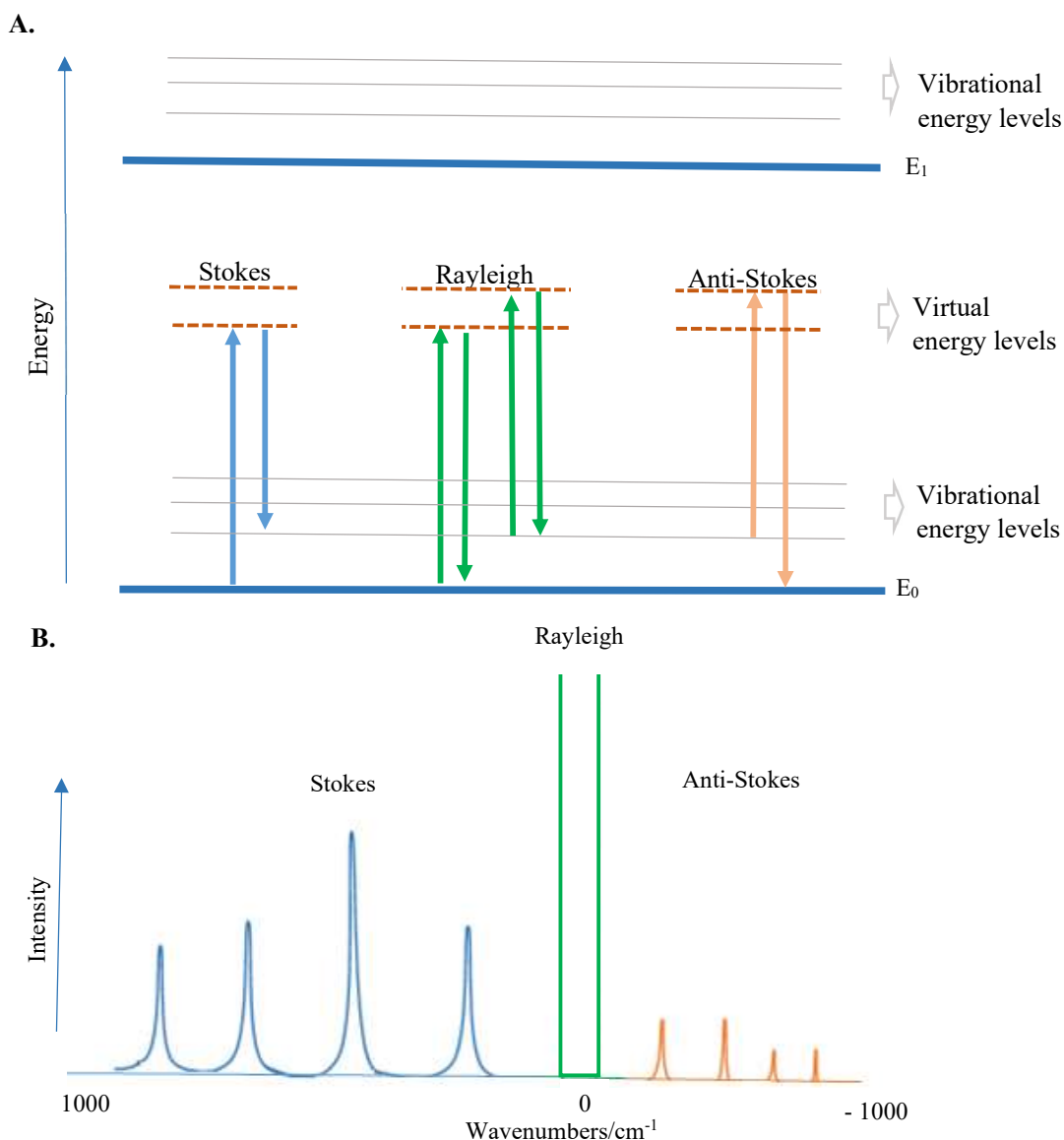


**Figure 1.** Energetic transitions involved in Raman scattering, **A.** More intense (blue shifted) Stokes bands, and less intense (orange shifted) anti-Stokes bands. Rayleigh line to higher wavenumbers (green shifted), without bands of Raman spectra, **B.**

excitation and filtering units for spectral purification. Typically, the characteristics of the devices vary depending on the size and relative cost of its components and accessories (5).

The diversity of the types of device configurations allows amplifying the sensitivity of the technique and allows a variety of applications, ranging from the quantification of drug substances in tablets and mixtures of powders to multiplex samples (3,10–17), samples in low concentrations (18,19), molecular traces (20–22), samples inside packs (23) and materials in nanometric scale (Table 1) (24,25).

Conventional Raman spectroscopy requires high sample concentration and it is affected by fluorescence. FT-Raman can resolve such spectral interference (11). Furthermore, fluorescence interference also can be reduced by exciting the near infrared laser sample as Nd-YAG at 1064 nm (5).

For samples at low concentrations, Resonance Raman Spectroscopy (RRS) increases the scattering sensitivity. In such cases, the samples must have electronic transitions close to the laser line's frequency. Thus, the incident radiation frequency coincides with an electronic transition of

the molecule, and as a result of this combination, a more intense Raman spectrum is obtained (18,19).

In the Surface-enhanced Raman spectroscopy (SERS), the sample is adsorbed on a colloidal metal surface or by nanostructures such as nanotubes typically made of gold (Au), silver (Ag) or copper (Cu) (20–22). This approach improves the intensity of signals and also extinguishes fluorescence.

Another variant, the Tip-enhanced Raman spectroscopy (TERS), provides high chemical sensitivity for surface molecular mapping with a nanoscale spatial resolution (24,25). This variant may help researchers to characterize and to develop nano-based strategies in innovative therapy. Furthermore, Micro-Raman presents a wide area of illumination, which allows overcoming the challenges of quantifying polymorphic mixtures (14).

All these variants were carefully developed aiming to overcome the limitations of the conventional Raman spectroscopy. By using chemometric treatments, it is possible to improve analytical models for the quantification of drugs substances and excipients in multicomponent formulas (10,16,26), as presented in Table 1.

### Raman calibration model

The interpretation of a complex spectrum of samples requires the use of chemometric calibration models. Chemometrics is the use of mathematical and statistical methods in chemical data, allowing the acquisition and extraction of essential information regarding the components of the formulation, as shown in Figure 2 (27). For this, it is necessary to apply a univariate or multivariate analysis.

The univariate analysis contemplates alone one variable at a time. Therefore, it uses a specific band intensity of the spectra (28). The multivariate analysis is a set of techniques that allows statistical analysis of data collected with more than one variable (29–32) such as the wavelengths and spectral interactions (33).

Due to the complexity and enormous amount of information acquired by Raman spectroscopy, it is uncertain whether univariate treatments are sufficient to select as the calibration model. Consequently, it is necessary to adopt multivariate analyses to understand and determine the relevance of the data originating from multiple variables (34–37).

The method most commonly used in the multivariate analysis is the partial least squares

(PLS) method (10,38,39), described by Wold in 1966 (40). Furthermore, for multicomponent matrices, classical least squares (CLS), alternating least squares (MCR), principal component regression (CRP), and principal component analysis (PCA) are commonly used (41).

For the development of the calibration models, carefully selected representative samples should be used, which generally require qualification by independent reference analytical procedures (36). The selection of these models depends on the type of data and analytical objectives. In some cases, to achieve better precision of the quantitative method, it is necessary to compare several multivariate models. Thus, it is possible to detect errors and allow selecting the appropriate model (41–43).

In 2015, the FDA (48) released the Analytical Procedures and Methods Validation for Drugs and Biologics Guidance for Industry. This guidance was harmonized with ICH to complement the guidance Q2(R1) Validation of Analytical Procedures: Text and Methodology (49). The guidelines provide the validation criteria to achieve a successful calibration model to support the quantitative analysis in pharmaceutical applications.

According to these official documents, to define a robust calibration model for quantification it is required the evaluation of the different sources of variability and includes them in the samples. These variabilities must be identified to predict and control them during method validation and routine application (36).

The performance characteristics for the spectroscopic methods is similar to the conventional ones and include the evaluation of accuracy, precision (repeatability and intermediate precision), specificity, linearity, range, and robustness (48,49). Besides, it is essential to use a referential method to validate the Raman spectroscopy method, usually the high-performance liquid chromatography method (HPLC). The reference values are necessary to determine the method accuracy (36,44).

In Table 2, the statistical parameters for the selection and prediction of the calibration model are presented. These are in accordance to the main performance characteristics established by the (48) and ICH (49). Bias refers to accuracy,  $Q^2$ ,  $Q_r$  and  $R^2$  assessing robustness, RMSEC, RMSECV and RMSEP refers to the quantitative performance of the calibration models.

Bias represents the systematic error and refers to accuracy, and this avoids the acceptance or

**Table 1.** Main variants of Raman spectroscopy for quantification

Variants	Brief description	Equipment Configuration	Advantages	Application	Ref
Conventional Raman scattering	Inelastic scattering effects responsible for generating different frequencies from the incident monochromatic light beam used to irradiate the sample.	Conventional equipment.	Non-destructive; Little or no sample preparation; Short analysis time.	API quantification and characterization of tablets.	(10)
Fourier transform-Raman (FT-Raman)	The spectrum is obtained from the Fourier transformed signal of the interfering light in a Michelson-type optical interferometer.	Multiplexing spectrometer system, such as a Michelson interferometer.	Measure all wavelengths simultaneously, improved sensitivity compared with the single channel spectrometers and less fluorescence interference.	API quantification in powder mixtures.	(3,11)
Transmission Raman spectroscopy (TRS)	'Unidirectional' mirror permitting the transfer of photons from one side and acting as a reflector for photons influencing it from the other side.	Photon diode or "unidirectional mirror".	Greater efficiency of laser photons in the sample; improved signal-to-noise ratio; improves the level of quantification accuracy.	Complex mixture containing different constituents at varying concentrations and quantitative analysis of pharmaceutical bilayer tablets.	(12,16)
Resonance Raman spectroscopy (RRS)	The incident photon energy approaches the electron transition energy.	Raman microscope.	Can investigate samples with low concentrations of single constituents or many different constituents.	Samples with low concentrations.	(18,19)
Surface enhanced Raman spectroscopy (SERS)	Amplification of electromagnetic fields generated by the excitation of localized surface plasmons.	Raman scattering by molecules adsorbed on rough metal surfaces or by nanostructures such as nanotubes typically made of gold (Au) or silver (Ag).	Sensitive and reliable method to determine the concentration of target molecules in unknown systems; Detect trace organic and inorganic analytes in different media in nanogram level.	Quantifies highly complex samples and target molecules in unknown systems.	(20–22)

Table 1 Continued

<b>Variants</b>	<b>Brief description</b>	<b>Equipment Configuration</b>	<b>Advantages</b>	<b>Application</b>	<b>Ref</b>
Spatially offset Raman spectroscopy (SORS)	Diffuse Raman scattering from a region away from the laser excitation. Uses the energy of vibrational motion from within a molecule.	Dedicated Raman microscopes or conventional equipment with a coupled microscope, which use optical fibers. Including handheld equipment.	Isolation of chemically rich spectral data from sub surfaces, substructures, layers and through other types of barriers. Quantifies chemical markers. Readings can penetrate container.	Samples inside packs and samples for medical diagnostics.	(9,23)
Coherent anti-Stokes Raman spectroscopy (CARS)	Non-linear optical imaging techniques, by means of non-linear probing of molecular vibrational resonances.	Inverted microscope with a laser-scanning confocal scan-head and photomultiplier tube (PMT) and GaAsP hybrid (HyD) photodetectors.	Label-free, chemically specific signal, fast data-acquisition time and inherent non-destructive “confocal”- like imaging.	Characterizes raw materials, tablets and powder mixtures.	(13,15)
Stimulated Raman Scattering (SRS)	Energy difference between the pump and Stokes photons matches the vibrational energy of the target molecules; the coherently induced vibrational transition absorbs one photon in the pump beam and gains one photon in the Stokes beam.	Visible stimulated Raman scattering microscope with dual-output laser system, a Stokes beam, and a pump beam.	Increased sensitivity, because it is free of limitations from labeling and applicable to spot reduction effect.	Characterizes multiple excipients distributions in tablets. Mapping of samples as cells and tissues.	(17)
Tip-enhanced Raman scattering (TERS)	Imaging involves measuring the signal at each pixel location of the corresponding scanning probe microscope image during the raster scan of the surface.	Raman spectroscopy coupled confocal microscope, and a scanning probe microscope.	Spatial resolution required for nanoscale characterization. Ability to spectroscopically map surfaces.	Characterization of materials at nanoscale.	(24,25)
Raman Micro spectroscopy (micro-Raman)	The sample is illuminated using laser light and an objective lens with a disc point size of 1µm in diameter or less.	Raman spectrophotometer coupled microscopes.	Acquire more representative spectra of the sample mixtures; The wide area illumination and/or reduced particle size allows for more accurate measurements of polymorphs.	Quantification of polymorphic mixtures, API content in tablets and powder mixtures.	(14)

API, Active Pharmaceutical Ingredient.

rejection of an inaccurate or capable method, respectively (44,45).  $Q^2$  represents the predictive capacity of the multivariate models, demonstrating the robustness evaluation; negative values indicate that the model is uncertain (10,46).  $Q_r$  represents variation usually from instrumental fault, and  $R^2$  is one of the most applied statistical parameters to determine sources of variation of the models (36,39).

In addition, RMSEC, RMSECV, and RMSEP refer to the prediction results of the validation method, the values of these parameters are dependent on the characteristics of the samples.

For example, in the color tablet coating analysis, the results depend on the model applied, but some colors lead to larger or smaller calibration errors (45). RMSECV is appropriate to test if the calibration model is well fitted according to the current data (35,36). RMSEP is the predictions of the calibration model; to satisfactory values, it is essential to consider matrix variations when comparing the predictive models (35,36,47). Therefore, these statistics e/or chemometric parameters (Table 2) allowing to make the assertive decision in Raman method validation.

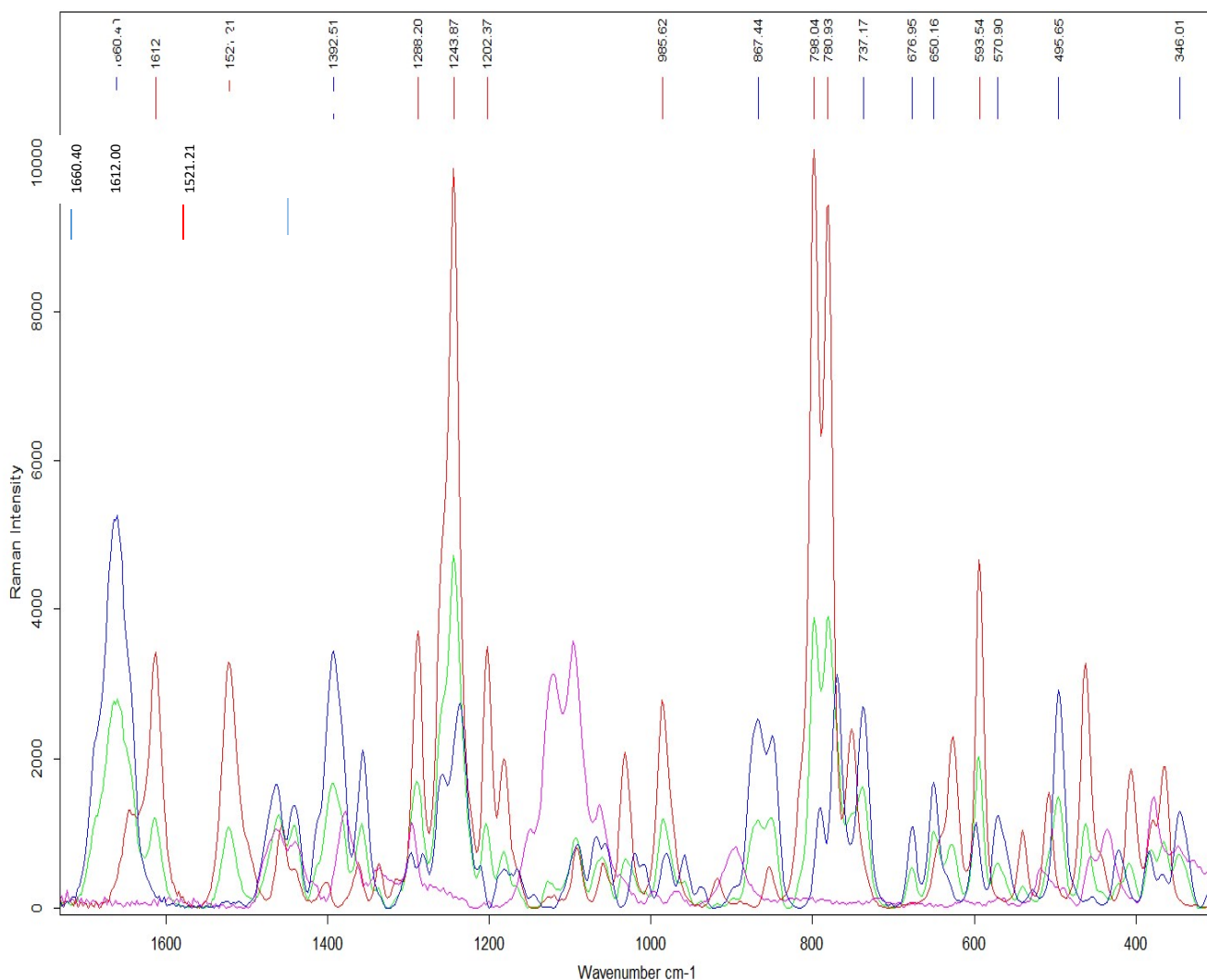


**Figure 2.** Raman spectra obtained by BRAVO Handheld Raman Spectrometer (Bruker Corporation, Billerica, MA, EUA). The analysis shows the ability of Raman spectroscopy to characterize specific bands of substances in the multi-component formula. The peaks arising at wavelengths 1660, 1392, 867, and 495 represents the antiretroviral zidovudine (blue spectrum). The red line (red spectrum) refers to lamivudine, commonly associated antiretroviral with zidovudine, for which the bands with intensity at wavelengths 1243, 798, and 780 are the most characteristic. The purple spectrum represents the mixture of excipients (microcrystalline cellulose, croscarmellose sodium, colloidal silicon dioxide, magnesium stearate, Opadry™ white YS-1-7003). Green spectrum represents the powder mixture of the formula components (lamivudine + zidovudine 150mg + 300mg); even in the complex mixture, it is possible to distinguish the main peaks of each drug and differentiate them from the excipients bands.

**Table 2.** Main statistical parameters for prediction multivariate analysis

Statistical parameters	Description	Formula	Meaning	Range	Reference value	References
Bias	Represents the systematic error, is the average value of the difference between predicted and measured values.	$Bias = \frac{\sum_{i=1}^n (y_i - \hat{y}_i)}{n} / \%$	$\hat{y}$ is the prediction value, y is the reference value and i is the test set sample.	0 - 1	Nearly zero.	(44,45)
Q <sup>2</sup>	Predictive Relevance: Represents the fraction of the total variation of the response that can be predicted by the model.	$Q^2 = 1.0 - PRESS / SS$	PRESS: prediction error sum of squares, the sum of squared differences between predicted and observed Y -data. SS: residual sum of squares of the previous components.	0 - 1	0 - 1	(10,46)
Q <sub>r</sub>	Sum of squared reconstruction error: determines whether a sample spectrum is different due to an un-modeled source of variance.	$Q_r = \text{sum}(x_i - t_i P^T)^2$	x <sub>i</sub> is the sample spectrum, t <sub>i</sub> is the latent variable scores for the sample spectrum, and P is the model loading.	0 - 1	0 - 1	(36,39)
R <sup>2</sup>	Coefficient of determination: is the proportion of the variance in the dependent variable predictable from the independent variable(s).	$R^2 = 1 - \frac{SS_{Regression}}{SS_{Total}}$	SS <sub>Regression</sub> : sum of squares regression. SS <sub>Total</sub> : total sum of squares.	0 - 1	1	(36,39)
RMSEC	Root mean square error of Calibration: Is the corresponding measure for the calibration model fit. Represents the proximity of the data of calibration model and samples data.	$RMSEC = \sqrt{\frac{\sum_{i=1}^n (y_i - \hat{y}_i)^2}{n}} / \%$	y <sub>i</sub> and $\hat{y}_i$ as the known and calculated mass of coating suspension in sample i and n as the number of samples.	Are determined by the measurement error in the reference values.	Depends on the reference value.	(45)

Table 2. Continuance

Statistical parameters	Description	Formula	Meaning	Range	Reference value	References
RMSECV	Root mean square error of cross-validation: Prediction errors are calculated for the samples left out as the difference between prediction and reference value.	$RMSECV = \sqrt{\frac{\sum_{i=1}^n (\hat{y}_i - y_i)^2}{n - 1}}$	$\hat{y}$ and $y$ represent vectors of predicted and reference values, respectively, and $n$ the number of samples.	Are determined by the measurement error in the reference values.	Depends on the reference value.	(35,36)
RMSEP	Root mean square error of prediction: deployed to quantify the uncertainty in all future predictions of the calibration model.	$RMSEP = \sqrt{\frac{\sum_{i=1}^n (\hat{y}_i - y_i)^2}{n}}$	$\hat{y}$ and $y$ represent vectors of predicted and reference values, respectively, and $n$ the number of samples.	Are determined by the measurement error in the reference values.	Depends on the reference value.	(35,47)

### Spectroscopy Raman in pharmaceutical development

In pharmaceutical development, a quality by design (QbD) approach is essential to identify the particularities of drug substances and excipients for new formulations (50–53). This concept allows risk management in the development of new medicines (54–58).

Raman spectroscopy allows for identifying critical variables and their clinical relevance related to quality and safety for patients (26,50,59,60). Table 3 presents 14 studies in the last five years, related to the use of this technique in the product development phase. In these studies, 23 drug substances from 10 therapeutic classes were evaluated.

Protasova and colleagues (61) demonstrated the applicability of Raman spectroscopy for monitoring reactions in solid phases (Table 3). They

describe its current applications in the synthesis of drug candidates. In the early developmental studies, this technique helps characterize the active pharmaceutical ingredient (API) and understand drug-excipient interactions in the formulation, besides allowing for evaluating the critical quality attributes of pharmaceutical products (CQAs) (62,63).

These attributes play a fundamental function in the quality, safety, and efficacy of pharmaceuticals, directly influencing the bioavailability of drugs (63–65). In this sense, 57% of the studies presented in Table 3 evaluated the crystalline and polymorphic forms of the compounds in mixtures of powders and commercial products.



Three different devices were compared: benchtop confocal microscope coupled spectrophotometer (micro-Raman1), portable spectrophotometer (macro-Raman1) and benchtop spectrophotometer (macro-Raman2) for the quantification of three polymorphs of mebendazole in mixtures (Table 3). Partial least squares regression models (PLS) were developed obtaining RMSEP values of 1.68%, 1.24% and 2.03% (w/w) for polymorphs A, B, and C, respectively, using the macro Raman analysis. This macro presented better performance, due to the configurations of this equipment, which provides more widely illuminated area laser, allowing getting more reproducible and representative spectra (14).

Similarly, for the quantification of crystalline and amorphous forms of warfarin sodium (Table 3) using PLS and PCR, the obtained values were:  $R^2 = 0.993$ , RMSEC = 2.60 and Bias = 0.007; and  $R^2 = 0.993$ , RMSEC = 2.61 and Bias = 0.019 for PLS and PCR, respectively (66). The predictive results for the quantification of the fraction of crystalline (theoretical 10%) and fraction amorphous (theoretical 90%) were  $15.32 \pm 2.63\%$  and  $84.68 \pm 2.63\%$ , respectively, for PLS and  $15.32 \pm 2.61\%$  and  $84.68 \pm 2.61\%$ , respectively, for PCR. These analyses are critical; especially in the case of formulation development with low therapeutic index drugs, in which any change in these forms over the life cycle of a product, can affect the performance of the drug adding risk to the patient (66).

The understanding of the crystalline forms of the drug substance and the interactions with the excipients are of fundamental importance for formulations in different presentations, mainly those exposed to humidity (53,64,65). Three of the 13 studies presented in Table 3 monitored the transition of the crystalline form (cocrystallization) allowing their in-line quantification. These demonstrated that the Raman technique is a reliable tool to solve challenges for the quantification of highly hygroscopic drugs (53,67,68).

Table 3 shows the particle size monitoring in 2 of 13 studies. The mean particle size of micronized components in the development of ebastine tablets (6.25 wt. %) was calculated using polystyrene microspheres as standard size ( $4.9 \pm 0.4$ ,  $9.8 \pm 0.5$  and  $15.8 \pm 0.6 \mu\text{m}$ ). The particle size and the forms of the components of the formulation remained unchanged throughout the tablet development process (28). Similarly, a Raman probe was used to evaluate changes in the size and shape of drug substance particles, generated from the friction in the powder mixing process (69).

Furthermore, Walker and colleagues (70) used the FT-Raman variant and Low-Frequency Raman Spectroscopy to identify disorders during the milling of the L-tryptophan and indomethacin drugs individually and in the binary mixture (1: 1 molar ratio). Analysis revealed that the blend changed more rapidly and more thoroughly compared to the separate components. Such phenomena indicated possible favorable intermolecular interactions between the two substances. These evaluations are critical for forecasting and planning large-scale production processes.

Interactions among the components and degradation products can be detected by Raman under adverse conditions such as temperature (71,72). SERS was employed (Table 1) for the quantification of ofloxacin and for monitoring its stability after several forced degradation processes. The studies revealed method capacity for quantifying this drug in the presence of its degradation product, simultaneously (73).

In addition, in the development stage, nine different software applications supported Raman analysis (Table 3). This software considers the main variables and statistical parameters applicable to multivariate analyses. Thus, they have a fundamental role in modeling, prediction, and optimization of the chemometric models. Therefore, they allow minimizing the exhaustive work for application and understanding of these calculations and formulas, in the development and routine analysis.

In pharmaceutical development, a quality by design (QbD) approach is essential to identify the particularities of drug substances and excipients in complex mixtures and in multi-component formulas and their clinical relevance. Raman spectroscopy, combined with multivariate models allows identifying the main critical variables, such as interactions between the drug substances and the other components and changes in the crystalline form of the drug. Thus, Raman spectroscopy plays a key role in risk management in the development of new medicines.

### **Raman spectroscopy in process analytical technology**

The CGMPs for the 21<sup>st</sup> Century (59), harmonized with the concept of QbD addressed by ICH (50), allows for understanding, continuous improvement and allows for reducing the variabilities in the critical stages of the process, ensuring higher quality to the final product (74).

**Table 3.** Raman spectroscopy in pharmaceutical development

Drug Substance	Therapeutic Classification	Excipients	Critical Quality Attributes	Variants	Equipment	Manufacturer	Calibration Model	Data Analysis Software	References
Mebendazole	Anthelmintic	Binary and ternary mixtures containing polymorphs.	Polymorph quantification in mixtures.	Raman microscopy	T64000 (micro-Raman1); TacTicID-GP (macro Raman1); RamanStation 400F (macro Raman2)	Horiba – Jobin Yvon; B&W Tek.; Perkin-Elmer	PLS, MSC, SNV, WLS	The Unscrambler X 10.3 (CAMO) and MATLAB R2010a (Math Works).	(14)
Ofloxacin	Antibiotic	Commercial dosage forms.	Forced degradation procedures in eye drop and tablets.	Surface-enhanced Raman spectroscopy (SERS)	Confocal Raman spectrometer LabRam HR800	Horiba Jobin Yvon, Bensheim, Germany.	Regression analysis and validation using ICH guidelines	Not mentioned	(73)
Warfarin sodium	Anticoagulants	Anhydrous lactose, pregelatinized starch, magnesium stearate, hydroxypropyl cellulose, methanol and deuterated water (99.9%).	Quantification of Crystalline/Amorphous API in mixtures (placebo and sample matrices).	Raman spectroscopy	RamanRXN2™ Multi-Channel Raman Analyzer	Kaiser Optical System Inc., Ann Arbor, Michigan.	PLS, PCR	Unscrambler X software (version10.1; Camo Software Inc., Woodbridge, New Jersey).	(66)
Carbamazepine/Nicotinamide	Anticonvulsant, Psychotropic and Neurotropic	Solvent (ethyl acetate) for crystallization reaction.	In-line monitoring of cocrystallization process and quantification in ternary mixture.	Raman spectroscopy	i-Raman BWS 415-785H	B&W Tek, Inc., Newark, DE, USA.	PCA, PLS, MCR-ALS	PLStoolbox 6.2 (Eigenvector Research Inc., Wenatchee, WA, USA); Matlab®2011a (Mathworks Inc., Natick, MA, USA).	(68)

Table 3. Continuance

Drug Substance	Therapeutic Classification	Excipients	Critical Quality Attributes	Variants	Equipment	Manufacturer	Calibration Model	Data Analysis Software	References
N-acetylbenzylamine and N-benzylethanethioamide	Antiepileptic	Not mentioned	Intermolecular interactions in Polycrystalline samples.	Confocal Raman Imaging	WITec confocal CRM alpha 300 Raman microscope	WITec Instruments Corp., Knoxville, TN. USA.	Analysis of crystallographic data.	WITec software (Project FOUR 4.1).	(71)
Ebastine	Antihistamine	Lactose, carmellose calcium, crystalline cellulose, hydroxypropyl cellulose, magnesium stearate and light anhydrous silicic acid.	Particle sizing.	Raman microscopy	Raman microscope: LabRAM	ARAMIS, Horiba, Kyoto, Japan.	Univariate analysis and Raman chemical images.	ISys 4.0 CI software (Malvern Instruments).	(28)
Furosemide/Nicotinamide	Antihypertensive	Ethanol, microcrystalline cellulose and hydroxypropyl cellulose.	Monitoring of cocrystals: the crystalline-form conversion in suspension or fluidized bed granulation.	Low-frequency (LF) Raman spectroscopy and Conventional Raman spectroscopy	THz-Raman® Probe System, TRPROBE and Raman RXN1 System	Ondax, Inc., CA, USA and Kaiser Optical Systems, Inc., MI, USA.	Calibration using sulfur.	HoloGRAMS 4.1 (Kaiser Optical Systems, Inc.).	(53)
L-tryptophan Indomethacin	Anti-inflammatory	Not mentioned	Identifying disorder during Milling.	FT-Raman/Low-Frequency Raman Spectroscopy	Multi-RAM FT-Raman spectrometer	Bruker Optics, Ettlingen, Germany.	PCA, SNV	Unscrambler X 10.3 (CAMO Software AS, Oslo, Norway).	(70)

Table 3. Continuance

Drug Substance	Therapeutic Classification	Excipients	Critical Quality Attributes	Variants	Equipment	Manufacturer	Calibration Model	Data Analysis Software	References
Celecoxib	Anti-inflammatory	Kollidon <sup>®</sup> 25 (PVP), magnesium stearate and sodium chloride.	Quantification of the solid-state properties of drugs in tablets.	Transmission Raman spectroscopy	Kaiser RXN1 Microprobe	Kaiser Optical Systems (Ann Arbor, MI, USA)	PLS	MatLab (Mathworks, Natick, MA, USA) and PLS Toolbox 8.1.1 (Eigenvector Research Inc. Manson, WA, USA).	(72)
Lamivudine	Anti-viral	H <sub>2</sub> O/ethanol solution for recrystallization.	Polymorphism and polymorphic transformation.	Fourier Transform Raman	FT-Raman spectrometer	Thermo Nicolet 960, USA.	Normalized relative peak areas and heating times with single exponential functions.	Not mentioned	(64)
Ezetimibe	lipid-lowering compounds	Croscarmellose, Lactose monohydrate, Magnesium stearate, Cellulose, and Povidone.	Monitoring crystalline phase transition of API and quantification in Powder of the mixture and tablets.	Raman spectroscopy	<i>i</i> -Raman BWS415-785H. (Portable equipment)	B & W Tek, Inc., Newark, DE, USA.	PCA, PLS, MCR-ALS	PLS tool box 6.2 (Eigenvector Research Inc., Wenatchee, WA, USA) and Matlab <sup>®</sup> 2011a (Mathworks Inc., Natick, MA, USA).	(67)

Table 3. Continuance

Drug Substance	Therapeutic Classification	Excipients	Critical Quality Attributes	Variants	Instrument	Manufacturer	Calibration Model	Data Analysis Software	References
Reaction molecular	Not mentioned	Sulfonyl chloride resin and Merrifield resin.	Monitoring reactions on solid phases.	Raman spectroscopy	Not mentioned	Not mentioned	Choice of functional groups and the implementation of a suitable model system.	Not mentioned	(61)
BMS-823778-03	Not mentioned	Lactose anhydrous, microcrystalline cellulose and magnesium stearate.	Particle size distributions in powder mixtures.	Raman microscopy	Kaiser Raman system	Kaiser Optical Systems Inc., Ann Arbor, USA	Comparison of the measured particle spectra with reference library spectra and classification of individual components.	MiniTab 15 (Minitab, State College, PA, USA), and SigmaPlot version 12.5 (Systat software Inc., Chicago, USA).	(69)

API: Active Pharmaceutical Ingredient. MCR: Multivariate Curve Resolution. MCR-ALS Multivariate Curve Resolution with Alternating Least Squares. MSC: Multiplicative Scatter Correction. PCA: Principal Component Analysis. PLS: Partial Least Squares. SNV: Standard Normal Variate. WLS: Weighted Least Squares.

Thus, in 2004 the FDA published the Guide to Process Analytical Technology (PAT), defined as a risk-based scientific approach, aimed at supporting innovation and efficiency in pharmaceutical development, manufacturing, and quality (75).

Real-time PAT analysis can be in-line/online, and it is carried out directly on the production line, in critical stages as in the process of mixing, granulation, and drying. At-line, rapid analyses are carried out, after the critical steps of the process, for example, spectroscopy and disintegration assay (50,76).

Raman spectroscopy allows for identifying changes in physicochemical properties during the relevant unitary operations from the pharmaceutical point of view. Such an approach enables real-time understanding of these

processes. Therefore, it has essential advantages as PAT tools, meeting regulatory requirements (33,46,53,77).

Riolo and colleagues (78) highlighted the importance of Raman spectroscopy monitoring in the early part of a production process. The acquisition of initial data is fundamental for statistical treatment and identification of variabilities, aiming to determine the outcome of powder mixtures and ensure the manufacture of safe and effective medicines. Additionally, other two studies of 13 (Table 3) presented real time monitoring of the powder mixing process. The drug substance quantification occurred during the process, which allowed for evaluating the mixing profiles, as well as identifying the outcome of these, ensuring their uniformity (78–80).

Two of three of these studies used the same model of the phantom (PhAT: Pharmaceutical Area Testing) with the same condition of excitation and diameter of point for quantification of the drugs, although with different types of equipment (79,80). These examples show that some accessories and devices can be applicable for different equipment configurations, including different manufacturers, as in a study performed by Netchacovitch and colleagues (33). In this study, a Kaiser Optical Systems probe coupled to a Perkin Elmer device was used. Table 3 revealed that 85% of the studies (11 of 13) used the equipment of the manufacturer Kaiser Optical Systems.

A single-channel device model, used for measurements through the glass wall of the mixer, allowed acetyl salicylic acid detection (1.1% w/w) in the evaluation of an aspirin mixture with Avicel PH-101, at a 50-rpm profile. The monitored variable was the drug substance particle size. The results did not identify profile variation in the mixture during the process. However, an increase in the time to obtain a homogeneous mixture was observed, through the evaluation of peak-to-peak noise of the spectra. This behavior was dependent on the drug substance concentration as they added the drug (79).

Unlike the previous study, a multichannel device was used to quantify drug substances in samples of powders and tablets employing simultaneous monitoring (PhAT probes) of the blend. The performance characteristics of the method revealed, coefficients of determination ( $R^2_c = 0.9695$ ,  $R^2_{cv} = 0.9605$ ), errors (RMSEC [% w/w] = 0.8295, RMSECV [% w/w] = 0.9446, RMSEP [% w/w]) = 0.8246 and  $Bias_{cv}$  [% w/w] = 0.0091, respectively. The real-time monitoring of the powder mixture allowed for indicating possible problems such as an insufficient amount of powder in the mixer and changes in the concentration of the API (80).

In addition, the Raman technique can be suitable in online monitoring of the gel mixing process. Predictive results for method performance ( $R^2 = 0.973$ ;  $Q^2 = 0.973$ ; RMSECV = 0.0418% w/w) were obtained even in a low concentration. On three different days, RMSEP values of 0.0255, 0.0235 and 0.0381% (w/w) for three validation sets were obtained (81). These results evidence the capability of the technique to evaluate the mixtures of different pharmaceutical forms (solid, semi-solid, and liquid). In addition, the Raman technique allows for quantifying samples with high water content, demonstrating its viability in the monitoring granulation unit operation (67,82,83).

The granulation process was monitored in 5 of 13 studies (Table 3) using the partial least squares (PLS) calibration model, which was applied in 100% of the cases, although two studies also used other methods such as MCR, PCA, and MLR.

With reference to these models, the MCR model was the only predictive model not to exceed the established acceptance limits of 10% (relative Bias) for the monitored mixtures containing 17.5, 22.5, 25.0, 27.5 and 32.5% (w/w) of metoprolol. The calibration model for the quantification of drug substances during the hot melt extrusion process presented results of accuracy, precision (95 of the 100 measurements below the predefined acceptance limits of 10%) and robustness (46).

The calibration models should consider the concentration of the drugs in the powder mixture, the time of exposure of the sample to radiation, and the volume of the sample. This volume shall not overstep three times the unit dose range (33,36,46,84).

Following the development of the appropriate PLS calibration model, Harting and Kleinebudde (84) demonstrated RMSEP of 0.59% and 1.5%, respectively, for the quantification of ibuprofen and diclofenac sodium. A difference of 6% in the concentration of diclofenac was observed due to not cleaning the granulator between the tests. This demonstrates the ability of the technique to identify variability and possible challenges in the processes, such as equipment setup failure.

Like the previous study, a univariate and a multivariate model (including all wavelengths and their interactions) were developed for quantification of itraconazole in line, for monitoring the hot-melt extrusion process. The validation for the two calibration models occurred; however, the multivariate approach was more accurate due to including a more significant number of variables in the model (33). Such an approach may justify the use of multivariate models in 100% of the studies presented in Table 3.

Five of 13 studies (Table 3) were developed for monitoring of the coating nuclei stages. Recently, Korasa and Vrečer (85) monitored the pellet coating process using an in-line probe. The results were  $R^2 = 0.9970$ , RMSEP = 0.5998 and slope of the regression line of 0.9463, which showed high consistency between observed and predicted values. The technique not only contains a tool to determine the amount of spray coating, but it is also able to assess the thickness of the coating (85).

Similarly, an MCR calibration model for the quantification of multilayer film coating was developed. The model allowed to predict the

thickness of films during the process and showed better performance compared to the PLS regression model, more frequently applied, as revealed in Table 3 (86).

Kim and Woo (87) evaluated coat weight gain in-line by quantitative analysis of the film layer. They accurately monitored the endpoints of the process with an aim weight gain of 3% (w/w). Image analysis was also performed on the coating layer, using a Raman microscope showing an increase of thickness.

Fluorescence from pigments or certain excipients may interfere with spectral analyses (87), although, two studies reported the sensitivity of the technique for monitoring the processes of colored coatings (Table 3). In the first study, in-line monitoring using multivariate models (PLS and SBC) and a univariate analysis model were developed for endpoint determination of the coating process of colorless suspension. The method evidenced to have high predictive power ( $R^2 = 0.9996$   $Q^2$  RMSEC/% = 0.85 and RMSEP/% = 0.96) and all spectral variation were linear over time (88).

In the second study, the authors monitored six colored coatings, which after 30 min of the process, there was no change, which revealed its endpoint. Such an approach allowed for reducing this step by 20 minutes (from 50 to 30 minutes) (45).

The ability of the continuous verification presented in these studies allows a greater understanding of the variabilities of the primary pharmaceutical unit operations. The potential to overcome the challenges of quantifying, in-line, samples in the presence of classical interferences from the pharmaceutical industry, such as fluorescent and highly hygroscopic components, is presented. Also, the ability to determine the endpoints of blending processes increases patient safety, reduces process time and open the way for continuous production and reduction of lead time release, one of the significant challenges of the pharmaceutical industries.

### **Raman spectroscopy in pharmaceutical nanomaterials**

Improvements in the technology used to obtain nanocrystals have presented opportunities never achieved before to facilitate the administration of medicines. This approach efficiently increases the surface area of the drug with the biological media and increases the saturation solubility. This

promoted an increase in dissolution rate and may increase bioavailability. In addition, it presents greater bioadhesiveness to the biological membranes compared to the drug in the micrometric scale. Such advantages potentially improve the safety and efficacy of the drugs, allowing dose reduction (89–92).

In recent decades, there has been a significant rise in the development of drug nanocrystals. As of 2017, more than 80 drug nanocrystal applications were submitted to the FDA (90). The critical attribute characteristics of drug nanocrystals such as size, particle-size distribution and mean particle diameter, along with morphological analyses are fundamental to evaluate crystalline forms and to optimize size-dependent properties (90,93,94).

Due to the versatility of Raman technology and the interface advantage of different analytical tools with this technique, they can lead to an expansion into the field of pharmaceutical nanotechnology (1). Surface Raman Enhanced Scattering (SERS) and Tip-enhanced Raman spectroscopy (TERS) (Table 1) enhance the sensitivity of the technique and enable the evaluation of nanoscale substances (21,24,25,95,96).

Low-frequency Raman spectroscopy was applied to evaluate the crystalline state of nanocrystals; the technique was able to assess the polymorphic form of furosemide after nano pulverization (89). In addition, this technique allowed chemical and spatial quantification in the process of mixing cellulose nanocrystals in thermoplastics (97).

A method for quantitative analysis of alginate nanocarriers loaded with curcumin in hydrogels presented standard deviation results of SD equal to 0.34, 0.50 and 0.96% (w/w) and relative error of 3.21, 0.42 and 0.85% for concentrations of 2.11, 5.43 and 10.48% (w/w), respectively, using the PLS predictive model. Due to low interference from samples with high water content, the precision of the method demonstrated the effectiveness of the technique for the quantification at low concentrations of nanocrystals (98).

Besides, Raman spectroscopy Raman spectroscopy was employed to characterize graphite oxide nanoparticles to aid the administration of photothermally-controlled drugs (99). It allowed evaluating the penetration capacity of caffeine and propylene glycol nanocrystals in gel form applied topically to swine (100). Furthermore, it enabled the broader verification of cellular interactions in cytotoxicity assays (101).

**Table 4.** Raman spectroscopy in pharmaceutical process measurements

Sample characteristic	Drug Substance	Unit Operations	Operating Principles	Instrument	Manufacturer	Accessories and apparatus	Calibration Model	Application/Critical Quality Attributes	References
Powder blending	Aspirin, aspartame, Avicel PH-101 and sodium nitrate.	Blending	Convection Mixing	Raman RXN1™	Kaiser Optical Systems Inc., Ann Arbor, MI, USA.	PhAT probe, excitation laser 785 nm and a spot size diameter of 6 mm.	PLS	<i>In situ</i> monitoring of powder blending	(79)
Powder blending	Confidential	Blending and Mixing	Diffusion Blending (Tumble)	Jobin Yvon Horiba LabRam confocal Raman spectrometer	Horiba, Kyoto, Japan.	Nd:YAG blue laser at 473.1 nm, and attached to an Olympus BX40 microscope.	Raman signal of the component of interest	Mixing monitoring	(78)
Powder blending and tablet	Anhydrous caffeine	Blending, granulation and tableting	Wet granulation and melt extrusion	RamanRxn2™ Hybrid	Kaiser Optical Systems, Ann Arbor, USA.	PhAT probe, excitation laser 785 nm spot size diameter of 6 mm and a Kaiser transmission accessory.	PLS	API content in blended powder and tablets in real-time	(80)
Gel (2% w/w) and Suspension (0.09% w/w)	confidential information	Mixing	Convection Mixing	RamanRxn2™ Spectrometer	Kaiser Optical Systems, Ann Arbor, MI, USA.	A CCD detector and a fiber-optic PhAT probe. Excitation laser 785 nm.	PLS	In-line quantitative determination (API) in a gel and suspension	(81)
Granules	Ibuprofen 50 and diclofenac sodium	Granulation	Twin-screw wet granulation	Raman RXN2™ Hybrid Analyzer	Kaiser Optical Systems, Ann Arbor, USA.	PhAT probe, excitation laser 785 nm and a spot size diameter of 6 mm.	PLS	In-line continuous API quantification	(84)
Extrudates	Itraconazole	Granulation	Hot-melt extrusion	RamanStation 400F	Perkin Elmer, MA, USA.	Raman probe (Kaiser Optical Systems Inc., MI, USA). Two-dimensional CCD detector.	PLS	API content in real-time during a Hot-Melt Extrusion process	(33)



Table 4. Continuance

Sample characteristic	Drug Substance	Unit Operations	Operating Principles	Instrument	Manufacturer	Accessories and apparatus	Calibration Model	Application/Critical Quality Attributes	References
Extrusion mixtures	Metoprolol tartrate	Granulation	Hot-melt extrusion	Raman Rxn1™ spectrometer	Kaiser Optical Systems, Ann Arbor, MI, USA.	Fiber-optic Raman Dynisco probe. Excitation laser 785 nm.	PLS, MCR	API content during pharmaceutical hot-melt extrusion	(46)
Tablet	Theophylline anhydrate	Granulation/ Unit Dosing	Wet High-Shear Granulation/ Tableting	RamanRxn2 Analyzer	Kaiser Optical Systems, MI, USA.	785 nm excitation laser, a CCD detector and PhAT probe (backscattering geometry). PhAT probe	PLS, PCA, MLR	Assessment and prediction of tablet properties	(77)
Pellets	Acetylsalicylic acid	Coating	Fluid-bed coating	RamanRXN2™ analyzer	Kaiser Optical Systems, USA).	using a diode laser operating at 785 nm	PLS, MCR, MCR-ALS, SNV, SVD	Coating thickness	(86)
Coated pellets	Diclofenac Sodium	Coating	Film Coating	RamanRXN1™ Spectrometer / HyperFlux™ PRO Plus Raman	Kaiser Optical Systems, Inc, USA / Tornado Spectral System, USA	PhAT probe with 785 nm excitation laser of 6 mm diameter / 785 nm laser.	PLS	Prediction of sprayed quantity, coating thickness, and Loss on drying.	(85)
Tablet	Coating excipients: detackifier, TiO <sub>2</sub> , Kolliphor® SLS, talc and aqueous film former that is polyvinyl alcohol	Coating	Pan Coating	a) Raman spectrometer b) Raman microscope	a) Kaiser Optical Inc., MI, USA. b) Nanophoton Corporation, Osaka, Japan.	a) 785nm diode laser and WAI probe having a spot size of 6 mm b) objective lens TU Plan Fluor 20x/NA0.45.	PLS	a) in-line monitoring for coating weight gain b) imaging analysis for coating layers and thickness	(87)
Tablet	Drug-free cores - Coating suspensions comprising polymers and	Coating	Gas Suspension	RamanRXN2™ Analyzer	Kaiser Optical Systems, Ann Arbor, USA.	PhAT probe, excitation laser 785 nm spot	PLS, MCR, SBC, UV	Endpoints of coating processes for colored tablets	(45)

	pigments and/or dyes					size diameter of 6 mm.			
Tablet	Placebo and caffeine cores	Coating	Gas Suspension	RamanRXN2™ Analyzer	Kaiser Optical Systems, Ann Arbor, USA.	PhAT probe, excitation laser 785 nm spot size diameter of 6 mm.	PLS, SBC, UV	Endpoint determination of a tablet coating process	(88)

API: Active Pharmaceutical Ingredient. MCR: Multivariate Curve Resolution. MCR-ALS Multivariate Curve Resolution with Alternating Least Squares. MLR: Multiple Linear Regression. NIPALS: Non-Linear Iterative Partial Least Squares. PCA: Principal Component Analysis. PCS: Principal Component Analysis. PLS: Partial Least Squares. PhAT: Pharmaceutical Area Testing. SBC: Science-Based Calibration. SNV: Standard Normal Variate. SVD: Singular Value Decomposition. WAI: Wide Area Illumination. UV: Univariate analysis.

Collectively, these studies highlight the prospects of routine analysis of materials at the nanometer scale, mainly, considering the possibility of auxiliary Raman spectroscopy and even replacing destructive techniques such as transmission electron microscopy, X-ray diffraction, and photoluminescence spectroscopy, commonly used for size analysis and nanocrystal characteristics.

### FINAL CONSIDERATIONS

The application of Raman spectroscopy has evolved due to its increasing instrumental versatility. This evolution allowed different configurations of the instrument, significantly improving its sensitivity. In combination with chemometric models, this technique makes it possible to investigate a wide variety of samples, quickly and non-destructively.

In the development of pharmaceutical products, this technique has been consolidated as a reliable quantitative analytical method in the evaluation of the main critical quality attributes. Raman spectroscopy has been able to overcome classic challenges of the pharmaceutical industry, such as the quantification of substances at low concentrations in complex mixtures, including the presence of their degradation products and in multicomponent

formulas of various therapeutic classes. Thus, it has become essential to identify critical variables and their clinical relevance in the development of new drugs in the QbD environment.

In process monitoring, this technique has been established for off-line measurements, but it is in real-time (in-line) control based on PAT, where it has advanced exponentially. In this sense, it allows quantification in powder mixtures under adverse conditions, as in the case of blends with high water content, semi-solid and liquid mixtures. It also enables the collection of an enormous amount of data, compared to the conventional technique by high-performance liquid chromatography. These data allow a greater understanding of variability in the pharmaceutical process, as well as the continuous verification of its critical stages and unit operations. Furthermore, it will enable researchers to overcome the challenges of quantifying, in-line, fluorescent interfering samples such as colored tablets.

Therefore, Raman spectroscopy has become a potent tool for pharmaceutical applications, integrated into the concept of Good Manufacturing Practices of the 21<sup>st</sup> Century. Recently, the use of Raman spectroscopy has advanced in pharmaceutical nanotechnology, standing out for quantifying materials on the nanoscale scale.

## ACKNOWLEDGEMENTS

We appreciate the support of Jim Hesson of Academic English Solutions.com, and Ana Paula Peinado of Bruker do Brasil Ltda., which provided us the BRAVO Handheld Raman Spectrometer.

## REFERENCES

- Paudel A, Rajjada D, Rantanen J. Raman spectroscopy in pharmaceutical product design. *Adv Drug Deliv Rev* 2015;89:3–20.
- Raman C V, Krishnan KS. The Optical Analogue of the Compton Effect. *Nature* 1928;121:377–8. 10.1038/121711a0.
- Zhu X, Xu T, Lin Q, Duan Y. Technical development of raman spectroscopy: From instrumental to advanced combined technologies. *Appl Spectrosc Rev* 2014;49:64–82. 10.1080/05704928.2013.798801.
- Depciuch J, Kaznowska E, Zawlik I, Wojnarowska R, Cholewa M, Heraud P, Cebulski J. Application of Raman Spectroscopy and Infrared Spectroscopy in the Identification of Breast Cancer. *Applied Spectrosc* 2016;70:251–63. 10.1177/0003702815620127.
- Bumrah GS, Sharma RM. Raman spectroscopy – Basic principle, instrumentation and selected applications for the characterization of drugs of abuse. *Egypt J Forensic Sci* 2016;6:209–215. 10.1016/j.ejfs.2015.06.001.
- Netchacovitch L, Thiry J, De Bleye C, Chavez PF, Krier F, Sacré PY, Evrard B, Hubert P, Ziemons E. Vibrational spectroscopy and microspectroscopy analyzing qualitatively and quantitatively pharmaceutical hot melt extrudates. *J Pharm Biomed Anal* 2015;113:21–33. 10.1016/j.jpba.2015.01.051.
- Wang H, Boraey MA, Williams L, Lechuga-Ballesteros D, Vehring R. Low-frequency shift dispersive Raman spectroscopy for the analysis of respirable dosage forms. *Int J Pharm* 2014;469:197–205. 10.1016/j.ijpharm.2014.04.058.
- Lakhwani GR, Sherikar OD, Mehta PJ. Nondestructive and rapid concurrent estimation of paracetamol and nimesulide in their combined dosage form using Raman spectroscopic technique. *Indian J Pharm Sci* 2013;75:211–6.
- Ember KJI, Hoeve MA, McAughtrie SL, Bergholt MS, Dwyer BJ, Stevens MM, Faulds K, Forbes SJ, Campbell CJ. Raman spectroscopy and regenerative medicine: a review. *NPJ Regen Med* 2017;2. 10.1038/s41536-017-0014-3.
- Casian T, Reznik A, Vonica-Gligor AL, Van Renterghem J, De Beer T, Tomuța I. Development, validation and comparison of near infrared and Raman spectroscopic methods for fast characterization of tablets with amlodipine and valsartan. *Talanta* 2017;167:333–343. 10.1016/j.talanta.2017.01.092.
- Dzsaber S, Negyedi M, Bernáth B, Gyüre B, Fehér T, Kramberger C, Pichler T, Simon F. A Fourier transform Raman spectrometer with visible laser excitation. *J Raman Spectrosc* 2015;46:327–332. 10.1002/jrs.4641.
- Griffen JA, Owen AW, Matousek P. Development of Transmission Raman Spectroscopy towards the in line, high throughput and non-destructive quantitative analysis of pharmaceutical solid oral dose. *Analyst* 2015;140:107–12. 10.1039/c4an01798f.
- Ojarinta R, Saarinen J, Strachan CJ, Korhonen O, Laitinen R. Preparation and characterization of multi-component tablets containing co-amorphous salts: Combining multimodal non-linear optical imaging with established analytical methods. *Eur J Pharm Biopharm* 2018;132:112–126. 10.1016/j.ejpb.2018.09.013.
- Paiva EM, da Silva VH, Poppi RJ, Pereira CF, Rohwedder JJR. Comparison of macro and micro Raman measurement for reliable quantitative analysis of pharmaceutical polymorphs. *J Pharm Biomed Anal* 2018;157:107–115. 10.1016/j.jpba.2018.05.010.
- Wu T, Chen K, Zhao H, Zhang W, Li Y, Wei H. Flexible dual-soliton manipulation for coherent anti-Stokes Raman scattering spectroscopy. *Opt Express* 2018;26:22001–22010. 10.1364/OE.26.022001.
- Zhang Y, McGeorge G. Quantitative Analysis of Pharmaceutical Bilayer Tablets Using Transmission Raman Spectroscopy. *J Pharm Innov* 2015;10:269–280. 10.1007/s12247-015-9223-8.
- Bi Y, Yang C, Chen Y, Yan S, Yang G, Wu Y, Zhang G, Wang P. Near-resonance enhanced label-free stimulated Raman scattering microscopy with spatial resolution near 130 nm. *Light Sci Appl* 2018;7. 10.1038/s41377-018-0082-1.
- Villegas Borrero NF, Clemente da Silva Filho JM, Ermakov VA, Marques FC. Silver nanoparticles produced by laser ablation for a study on the effect of SERS with low laser power on N719 dye and Rhodamine-B. *MRS Advances* 2019;4:723–731. 10.1557/adv.2019.157.
- Höhl M, Roth B, Morgner U, Meinhardt-Wollweber M. Efficient procedure for the measurement of pre-resonant excitation profiles in UV Raman spectroscopy. *Rev Sci Instrum* 2017;88. 10.1002/9781118971147.ch20.
- Chruszcz-Lipska K, Jaworska A, Szczurek E, Baranska M. (-)-R-mevalonolactone studied by ROA and SERS spectroscopy. *Chirality* 2014;26:453–61. 10.1002/chir.22288.
- Saleh TA, Al-Shalalfeh MM, Al-Saadi AA. Graphene Dendrimer-stabilized silver nanoparticles for detection of methimazole using Surface-enhanced Raman scattering with computational assignment. *Sci Rep* 2016;6. 10.1038/srep32185.
- Zong C, Xu M, Xu LJ, Wei T, Ma X, Zheng XS, Hu R, Ren B. Surface-Enhanced Raman

- Spectroscopy for Bioanalysis: Reliability and Challenges. *Chem Rev* 2018;118:4946-4980. 10.1021/acs.chemrev.7b00668.
23. Ellis DI, Eccles R, Xu Y, Griffen J, Muhamadali H, Matousek P, Goodall I, Goodacre R. Through-container, extremely low concentration detection of multiple chemical markers of counterfeit alcohol using a handheld SORS device. *Sci Rep* 2017;7. 10.1038/s41598-017-12263-0.
  24. Sonntag MD, Pozzi EA, Jiang N, Hersam MC, Duyn RP Van. Recent Advances in Tip-Enhanced Raman Spectroscopy. *J Phys Chem Lett* 2014;5:3125–30. 10.1021/jz5015746.
  25. Su W, Kumar N, Krayev A, Chaigneau M. In situ topographical chemical and electrical imaging of carboxyl graphene oxide at the nanoscale. *Nat Commun* 2018;9. 10.1038/s41467-018-05307-0.
  26. Kornecki M, Strube J. Process Analytical Technology for Advanced Process Control in Biologics Manufacturing with the Aid of Macroscopic Kinetic Modeling. *Bioengineering* 2018;5. 10.3390/bioengineering5010025.
  27. Hopke PK. The evolution of chemometrics. *Anal Chim Acta* 2003;500:365-377. 10.1016/S0003-2670(03)00944-9.
  28. Kuriyama A, Ozaki Y. Assessment of Active Pharmaceutical Ingredient Particle Size in Tablets by Raman Chemical Imaging Validated using Polystyrene Microsphere Size Standards. *AAPS PharmSciTech* 2014;15:375–87. 10.1208/s12249-013-0064-9.
  29. Petty RE, Laxer RM, Lindsley CB, Wedderburn LR. *Textbook of pediatric rheumatology*. 7th ed. Philadelphia: Saunders, 2016.
  30. Grimnes S, Martinsen ØG. *Bioimpedance and Bioelectricity Basics*. 3rd ed. Cambridge, Massachusetts: Academic Press, 2015.
  31. Nosyk B, Montaner JSG, Colley G, Lima VD, Chan K, Heath K, Yip B, Samji H, Gilbert M, Barrios R, Gustafson R, Hogg RS; STOP HIV/AIDS Study Group. The cascade of HIV care in British Columbia, Canada, 1996-2011: A population-based retrospective cohort study. *Lancet Infect Dis* 2014;14:40–9. 10.1016/S1473-3099(13)70254-8.
  32. Long FH. Multivariate Analysis for Metabolomics and Proteomics Data. In: Haleem JI, Timothy D V, editor. *Proteomic and Metabolomic Approaches to Biomarker Discovery*. Cambridge, Massachusetts: Academic Press, 2013, p. 299–311. 10.1016/B978-0-12-394446-7.00019-4.
  33. Netchacovitch L, Thiry J, De Bleye C, Dumont E, Cailletaud J, Sacré PY, Evrard B, Hubert P, Ziemons E. Global approach for the validation of an in-line Raman spectroscopic method to determine the API content in real-time during a hot-melt extrusion process. *Talanta* 2017;171:45–52. 10.1016/j.talanta.2017.04.060.
  34. Açıköz G, Hamamci B, Yıldız A. Determination of ethanol in blood samples using partial least square regression applied to surface enhanced raman spectroscopy. *Toxicol Res* 2018;34:127-132. 10.5487/TR.2018.34.2.127.
  35. Faber NM, Song XH, Hopke PK. Sample-specific standard error of prediction for partial least squares regression. *Trends Analyt Chem* 2003;22:330-334. 10.1016/S0165-9936(03)00503-X.
  36. Hossain MN, Igne B, Anderson CA, Drennen JK. Influence of moisture variation on the performance of Raman spectroscopy in quantitative pharmaceutical analyses. *J Pharm Biomed Anal* 2019;164:528-535. 10.1016/j.jpba.2018.10.022.
  37. Lavine BK. Special Issue: Chemometrics. *Appl Spectrosc* 2018;72:339. 10.1177/0003702818761619.
  38. Brouckaert D, Uyttersprot JS, Broeckx W, De Beer T. Development and validation of an at-line fast and non-destructive Raman spectroscopic method for the quantification of multiple components in liquid detergent compositions. *Anal Chim Acta* 2016;941:26–34. 10.1016/j.aca.2016.08.050.
  39. Wold S, Sjöström M, Eriksson L. *J Chemom* 2001;58:109-130. 10.1016/S0169-7439(01)00155-1.
  40. Wold H. Estimation of principal components and related models by iterative least squares. *Multivariate Analysis* 1966:1391–420.
  41. Farkas A, Vajna B, Söti PL, Nagy ZK, Pataki H, Van Der Gucht F, Marosi G. Comparison of multivariate linear regression methods in micro-Raman spectrometric quantitative characterization. *J Raman Spectrosc* 2015;46:566–76. 10.1002/jrs.4672.
  42. Fransson M, Johansson J, Sparén A, Svensson O. Comparison of multivariate methods for quantitative determination with transmission Raman spectroscopy in pharmaceutical formulations. *J Chemom* 2010;24:674–80. 10.1002/cem.1330.
  43. Singh VD, Daharwal SJ. Development and validation of multivariate calibration methods for simultaneous estimation of Paracetamol, Enalapril maleate and hydrochlorothiazide in pharmaceutical dosage form. *Spectrochim Acta A Mol Biomol Spectrosc* 2017;171:369–75. 10.1016/j.saa.2016.08.028.
  44. Müller J, Knop K, Wirges M, Kleinebudde P. Validation of Raman spectroscopic procedures in agreement with ICH guideline Q2 with considering the transfer to real time monitoring of an active coating process. *J Pharm Biomed Anal* 2010;53:884-94. 10.1016/j.jpba.2010.06.016.
  45. Barimani S, Kleinebudde P. Monitoring of tablet coating processes with colored coatings. *Talanta* 2018;178:686–97. 10.1016/j.ejpb.2017.05.011.
  46. Saerens L, Segher N, Vervae C, Remon JP, De Beer T. Validation of an in-line Raman spectroscopic method for continuous active pharmaceutical ingredient quantification during pharmaceutical hot-melt extrusion. *Anal Chim Acta* 2014;806:180–7. 10.1016/j.aca.2013.11.020.
  47. Sparén A, Hartman M, Fransson M, Johansson J, Svensson O. Matrix effects in quantitative assessment of pharmaceutical tablets using

- transmission raman and near-infrared (NIR) Spectroscopy. *Appl Spectrosc* 2015;69:580–9. 10.1366/14-07645.
48. Food and Drug Administration (FDA). *Analytical Procedures and Methods Validation for Drugs and Biologics*. Silver Spring, MD: FDA, 2015. Available at: <https://www.fda.gov/media/87801/download>. Accessed April 27, 2019.
  49. International Conference on Harmonisation of Technical Requirements for Registration of Pharmaceuticals for Human Use (ICH). *Validation of Analytical Procedures: Text and Methodology Q2(R1)*. 2005. Available at: [https://www.ich.org/fileadmin/Public\\_Web\\_Site/ICH\\_Products/Guidelines/Quality/Q2\\_R1/Step4/Q2\\_R1\\_Guideline.pdf](https://www.ich.org/fileadmin/Public_Web_Site/ICH_Products/Guidelines/Quality/Q2_R1/Step4/Q2_R1_Guideline.pdf). Accessed April 27, 2019.
  50. International Conference on Harmonisation of Technical Requirements for Registration of Pharmaceuticals for Human Use (ICH). *Pharmaceutical Development Q8(R2)*. 2009. Available at: [https://www.ich.org/fileadmin/Public\\_Web\\_Site/ICH\\_Products/Guidelines/Quality/Q8\\_R1/Step4/Q8\\_R2\\_Guideline.pdf](https://www.ich.org/fileadmin/Public_Web_Site/ICH_Products/Guidelines/Quality/Q8_R1/Step4/Q8_R2_Guideline.pdf). Accessed May 20, 2019.
  51. Kushner J, Langdon BA, Hiller JI, Carlson GT. Examining the impact of excipient material property variation on drug product quality attributes: A quality-by-design study for a roller compacted, immediate release tablet. *J Pharm Sci* 2011;100:2222-39. 10.1002/jps.22455.
  52. Kushner J, Langdon BA, Hicks I, Song D, Li F, Kathiria L, Kane A, Ranade G, Agarwal K. A quality-by-design study for an immediate-release tablet platform: Examining the relative impact of active pharmaceutical ingredient properties, processing methods, and excipient variability on drug product quality attributes. *J Pharm Sci* 2014;103:527-38. 10.1002/jps.23810.
  53. Otaki T, Tanabe Y, Kojima T, Miura M, Ikeda Y, Koide T, Fukami T. In situ monitoring of cocrystals in formulation development using low-frequency Raman spectroscopy. *Int J Pharm* 2018;542:56-65. 10.1016/j.ijpharm.2018.03.008.
  54. Aksu B, De Beer T, Folestad S, Ketolainen J, Lindén H, Lopes JA, de Matas M, Oostra W, Rantanen J, Weimer M. Strategic funding priorities in the pharmaceutical sciences allied to Quality by Design (QbD) and Process Analytical Technology (PAT). *Eur J Pharm Sci* 2012;47:402-5. 10.1016/j.ejps.2012.06.009.
  55. Li MY, Ebel B, Paris C, Chauchard F, Guedon E, Marc A. Real-time monitoring of antibody glycosylation site occupancy by in situ Raman spectroscopy during bioreactor CHO cell cultures. *Biotechnol Prog* 2018;34:486-493. 10.1002/btpr.2604.
  56. Santos RM, Kessler JM, Salou P, Menezes JC, Peinado A. Monitoring mAb cultivations with in-situ raman spectroscopy: The influence of spectral selectivity on calibration models and industrial use as reliable PAT tool. *Biotechnol Prog* 2018;34:659-670. 10.1002/btpr.2635.
  57. Bostijn N, Dhondt W, Vervaeke C, De Beer T. PAT-based batch statistical process control of a manufacturing process for a pharmaceutical ointment. *Eur J Pharm Sci* 2019;136. 10.1016/j.ejps.2018.02.007.
  58. Webster TA, Hadley BC, Hilliard W, Jaques C, Mason C. Development of generic raman models for a GS-KOTM CHO platform process. *Biotechnol Prog* 2018;34:730-737. 10.1002/btpr.2633.
  59. Food and Drug Administration (FDA). *Pharmaceutical CGMPs for the 21<sup>st</sup> Century - A risk-based approach*. Silver Spring, MD: FDA; 2004. Available at: <https://www.fda.gov/media/77391/download>. Accessed June 10, 2019.
  60. Wang X, Esquerre C, Downey G, Henihan L, O'Callaghan D, O'Donnell C. Assessment of infant formula quality and composition using Vis-NIR, MIR and Raman process analytical technologies. *Talanta* 2018;183:320–8. 10.1016/j.talanta.2018.02.080.
  61. Protasova I, Heissler S, Jung N, Braese S. Monitoring Reactions on Solid Phases with Raman Spectroscopy. *Chemistry* 2017;23:8703–11. 10.1002/chem.201700907.
  62. Dharani S, Rahman Z, Barakh Ali SF, Afroz H, Khan MA. Quantitative estimation of phenytoin sodium disproportionation in the formulations using vibration spectroscopies and multivariate methodologies. *Int J Pharm* 2018;539:65-74. 10.1016/j.ijpharm.2018.01.005.
  63. Yu LX, Amidon G, Khan MA, Hoag SW, Polli J, Raju GK, Woodcock J. Understanding Pharmaceutical Quality by Design. *AAPS J* 2014;16:771-83. 10.1208/s12248-014-9598-3.
  64. Du Y, Zhang H, Xue J, Tang W, Fang H, Zhang Q, Li Y, Hong Z. Vibrational spectroscopic study of polymorphism and polymorphic transformation of the anti-viral drug lamivudine. *Spectrochim Acta A Mol Biomol Spectrosc* 2015;137:1158-63. 10.1016/j.saa.2014.08.128.
  65. Izutsu K, Koide T, Takata N, Ikeda Y, Ono M, Inoue M, Fukami T, Yonemochi E. Characterization and Quality Control of Pharmaceutical Cocrystals. *Chem Pharm Bull* 2016;64:1421-1430. 10.1248/cpb.c16-00233.
  66. Rahman Z, Mohammad A, Akhtar S, Siddiqui A, Korang-Yeboah M, Khan MA. Chemometric Model Development and Comparison of Raman and <sup>13</sup>C Solid-State Nuclear Magnetic Resonance-Chemometric Methods for Quantification of Crystalline/Amorphous Warfarin Sodium Fraction in the Formulations. *J Pharm Sci* 2015;104:2550-8. 10.1002/jps.24524.
  67. Farias MA dos S, Soares FLF, Carneiro RL. Crystalline phase transition of ezetimibe in final product, after packing, promoted by the humidity of excipients: Monitoring and quantification by

- Raman spectroscopy. *J Pharm Biomed Anal* 2016;121:209-214. 10.1016/j.jpba.2016.01.008.
68. Soares FLF, Carneiro RL. In-line monitoring of cocrystallization process and quantification of carbamazepine-nicotinamide cocrystal using Raman spectroscopy and chemometric tools. *Spectrochim Acta A Mol Biomol Spectrosc* 2017;180:1-8. 10.1016/j.saa.2017.02.045.
69. Gamble JF, Hoffmann M, Hughes H, Hutchins P, Tobyn M. Monitoring process induced attrition of drug substance particles within formulated blends. *Int J Pharm* 2014;470:77-87. 10.1016/j.ijpharm.2014.04.028.
70. Walker G, Römann P, Poller B, Löbmann K, Grohganz H, Rooney JS, Huff GS, Smith GPS, Rades T, Gordon KC, Strachan CJ, Fraser-Miller SJ. Probing Pharmaceutical Mixtures during Milling: The Potency of Low-Frequency Raman Spectroscopy in Identifying Disorder. *Mol Pharm* 2017;14:4675-84. 10.1021/acs.molpharmaceut.7b00803.
71. Śmiszek-Lindert WE, Chelmecka E, Lindert O, Dudzińska A, Kaczmarczyk-Sedlak I. Towards a better comprehension of interactions in the crystalline N-acetylbenzylamine and its sulphur analogue N-benzyl-ethanethioamide. IR, Raman, DFT studies and Hirshfeld surfaces analysis. *Spectrochim Acta A Mol Biomol Spectrosc* 2018;201:328-338. 10.1016/j.saa.2018.05.021.
72. Edinger M, Knopp MM, Kerdoncuff H, Rantanen J, Rades T, Löbmann K. Quantification of microwave-induced amorphization of celecoxib in PVP tablets using transmission Raman spectroscopy. *Eur J Pharm Sci* 2018;117:62-67. 10.1016/j.ejps.2018.02.012.
73. El-Zahry MR, Lendl B. Structure elucidation and degradation kinetic study of Ofloxacin using surface enhanced Raman spectroscopy. *Spectrochim Acta A Mol Biomol Spectrosc* 2018;193:63-70. 10.1016/j.saa.2017.12.007.
74. Holm P, Allesø M, Bryder MC, Holm R. Q8(R2). ICH Quality Guidelines. In: Andrew T, David E, Raymond W N, editor. *ICH Quality Guidelines: An Implementation Guide*. Hoboken: John Wiley & Sons, Inc. 2017, p. 535-577. 10.1002/9781118971147.ch20.
75. Food and Drug Administration (FDA). Guidance for industry: PAT — a framework for innovative pharmaceutical development, manufacturing, and quality assurance. Rockville, MD: FDA; 2004. Available at: <https://www.fda.gov/media/71012/download>. Accessed Jun 15, 2019.
76. Esmonde-White KA, Cuellar M, Uerpmann C, Lenain B, Lewis IR. Raman spectroscopy as a process analytical technology for pharmaceutical manufacturing and bioprocessing. *Anal Bioanal Chem* 2017;409:637-49. 10.1007/s00216-016-9824-1.
77. Peeters E, Tavares da Silva AF, Toiviainen M, Van Renterghem J, Verduyck J, Juuti M, Lopes JA, De Beer T, Vervaeke C, Remon JP. Assessment and prediction of tablet properties using transmission and backscattering Raman spectroscopy and transmission NIR spectroscopy. *Asian Journal of Pharmaceutical Sciences* 2016;11:547-58. 10.1016/j.ajps.2016.04.004.
78. Riolo D, Piazza A, Cottini C, Serafini M, Lutero E, Cuoghi E, Gasparini L, Botturi D, Marino IG, Aliatis I, Bersani D, Lottici PP. Raman spectroscopy as a PAT for pharmaceutical blending: Advantages and disadvantages. *J Pharm Biomed Anal* 2018;149:329-34. 10.1016/j.jpba.2017.11.030.
79. Allan P, Bellamy LJ, Nordon A, Littlejohn D, Andrews J, Dallin P. In situ monitoring of powder blending by non-invasive Raman spectrometry with wide area illumination. *Journal of Pharmaceutical and Biomedical Analysis* 2013;76:28-35. 10.1016/j.jpba.2012.12.003.
80. Nagy B, Farkas A, Gyürkés M, Komaromy-Hiller S, Démuth B, Szabó B, Nusser D, Borbás E, Marosi G, Nagy ZK. In-line Raman spectroscopic monitoring and feedback control of a continuous twin-screw pharmaceutical powder blending and tableting process. *Int J Pharm* 2017;530:21-9. 10.5650/jos.ess13082.
81. Bostijn N, Hellings M, Van Der Veen M, Vervaeke C, De Beer T. In-line UV spectroscopy for the quantification of low-dose active ingredients during the manufacturing of pharmaceutical semi-solid and liquid formulations. *Anal Chim Acta* 2018;1013:54-62. 10.1016/j.aca.2018.02.007.
82. Griffen J, Owen AW, Matousek P. Development of Transmission Raman Spectroscopy towards the in line, high throughput and non-destructive quantitative analysis of pharmaceutical solid oral dose. *Analyst* 2015;140:107-12. 10.1039/c4an01798f.
83. Mazurek S, Szostak R. Quantification of active ingredients in pharmaceutical suspensions by FT Raman spectroscopy. *Vibrational Spectroscopy* 2017;93:54-64. 10.1016/j.vibspec.2017.10.003.
84. Harting J, Kleinebudde P. Development of an in-line Raman spectroscopic method for continuous API quantification during twin-screw wet granulation. *Eur J Pharm Biopharm* 2018;125:169-81. 10.1016/j.ejpb.2018.01.015.
85. Korasa K, Vrečer F. A study on the applicability of multiple process analysers in the production of coated pellets. *Int J Pharm* 2019;560:261-272. 10.1016/j.ijpharm.2019.01.069.
86. Hisazumi J, Kleinebudde P. In-line monitoring of multi-layered film-coating on pellets using Raman spectroscopy by MCR and PLS analyses. *Eur J Pharm Biopharm* 2017; 114:194-201. 10.1016/j.ejpb.2017.01.017.
87. Kim B, Woo YA. Coating process optimization through in-line monitoring for coating weight gain using Raman spectroscopy and design of experiments. *J Pharm Biomed Anal* 2018;154:278-84. 10.1016/j.jpba.2018.03.001.

88. Barimani S, Kleibudde P. Evaluation of in-line Raman data for end-point determination of a coating process: Comparison of Science-Based Calibration, PLS-regression and univariate data analysis. *Eur J Pharm Biopharm* 2017;119:28-35. 10.1016/j.ejpb.2017.05.011.
89. Barbosa SF, Takatsuka T, Tavares GD, Araújo GLB, Wang H, Vehring R, Löbenberg R, Bou-Chacra NA. Physical-chemical properties of furosemide nanocrystals developed using rotation revolution mixer. *Pharm Dev Technol* 2016;21:812-822. 10.3109/10837450.2015.1063650.
90. Chen M-L, John M, Lee SL, Tyner KM. Development Considerations for Nanocrystal Drug Products. *AAPS J* 2017;19:642-651. 10.1208/s12248-017-0064-x.
91. Davis BM, Pahlitzsch M, Guo L, Balendra S, Shah P, Ravindran N, Malaguarnera G, Sisa C, Shamsher E, Hamze H, Noor A, Sornsute A, Somavarapu S, Cordeiro MF. Topical Curcumin Nanocarriers are Neuroprotective in Eye Disease. *Sci Rep* 2018;8. 10.1038/s41598-018-29393-8.
92. Tyner KM, Zheng N, Choi S, Xu X, Zou P, Jiang W, Guo C, Cruz CN. How Has CDER Prepared for the Nano Revolution? A Review of Risk Assessment, Regulatory Research, and Guidance Activities. *AAPS J* 2017;19:1071-1083. 10.1208/s12248-017-0084-6.
93. Doğan I, Van De Sanden MCM. Direct characterization of nanocrystal size distribution using Raman spectroscopy. *J Appl Phys* 2013;114. 10.1063/1.4824178.
94. Doğan İ, van de Sanden MCM. Characterization of Nanocrystal Size Distribution using Raman Spectroscopy with a Multi-particle Phonon Confinement Model. *J Vis Exp* 2015. 10.3791/53026.
95. Hong S, Li X. Optimal Size of Gold Nanoparticles for Surface-Enhanced Raman Spectroscopy under Different Conditions. *J Nanomater* 2013;2013. 10.1155/2013/790323.
96. Xu X, Li H, Hasan D, Ruoff RS, Wang AX, Fan DL. Near-field enhanced plasmonic-magnetic bifunctional nanotubes for single cell bioanalysis. *Adv Funct Mater* 2013;23:4332-8. 10.1002/adfm.201203822.
97. Lewandowska AE, Eichhorn SJ. Quantification of the degree of mixing of cellulose nanocrystals in thermoplastics using Raman spectroscopy. *J Raman Spectrosc* 2016;47: 1337-1342. 10.1002/jrs.4966.
98. Miloudi L, Bonnier F, Bertrand D, Byrne HJ, Perse X, Chourpa I, Munnier E. Quantitative analysis of curcumin-loaded alginate nanocarriers in hydrogels using Raman and attenuated total reflection infrared spectroscopy. *Anal Bioanal Chem* 2017; 409:4593-4605. 10.1007/s00216-017-0402-y.
99. Chen J, Liu H, Zhao C, Qin G, Xi G, Li T, Wang X, Chen T. One-step reduction and PEGylation of graphene oxide for photothermally controlled drug delivery. *Biomaterials* 2014;35:4986-95. 10.1016/j.biomaterials.2014.02.032.
100. Mujica Ascencio S, Choe CS, Meinke MC, Müller RH, Maksimov G V., Wigger-Alberti W, Lademann J, Darvin ME. Confocal Raman microscopy and multivariate statistical analysis for determination of different penetration abilities of caffeine and propylene glycol applied simultaneously in a mixture on porcine skin ex vivo. *Eur J Pharm Biopharm* 2016;104:51-8. 10.1016/j.ejpb.2016.04.018.
101. Kuku G, Saricam M, Akhatova F, Danilushkina A, Fakhruddin R, Culha M. Surface-Enhanced Raman Scattering to Evaluate Nanomaterial Cytotoxicity on Living Cells. *Anal Chem* 2016;88:9813-20. 10.1021/acs.analchem.6b02917.